Molecular Biology of the Cell
Vol. 19, 5143–5155, December 2008

The Cardiolipin Transacylase, Tafazzin, Associates with Two Distinct Respiratory Components Providing Insight into Barth Syndrome

Steven M. Claypool,* Pinmanee Boontheung,* J. Michael McCaffery,† Joseph A. Loo,*‡§ and Carla M. Koehler*§

*Department of Chemistry and Biochemistry, ‡Department of Biological Chemistry, David Geffen School of Medicine, and the §Molecular Biology Institute, University of California, Los Angeles, CA 90095-1569; and †Integrated Imaging Center, Department of Biology, Johns Hopkins University, Baltimore, MD 21218-2685

Submitted September 2, 2008; Accepted September 9, 2008
Monitoring Editor: Janet M. Shaw

Mutations in the mitochondrial cardiolipin (CL) transacylase, tafazzin (Taz1p), result in the X-linked cardioskeletal myopathy, Barth syndrome (BTHS). The mitochondria of BTHS patients exhibit variable respiratory defects and abnormal cristae ultrastructure. The biochemical basis for these observations is unknown. In the absence of its target phospholipid, CL, a very large Taz1p complex is missing, whereas several discrete smaller complexes are still observed. None of the identified Taz1p complexes represents Taz1p homodimers. Instead, yeast Taz1p physically assembles in several protein complexes of distinct size and composition. The ATP synthase and AAC2, both required for oxidative phosphorylation, are identified in separate stable Taz1p complexes. In the absence of CL, each interaction is still detected albeit in reduced abundance compared with when CL is present. Taz1p is not necessary for the normal expression of AAC2 or ATP synthase subunits or assembly of their respective complexes. In contrast, the largest Taz1p complex requires assembled ATP synthase and CL. Mitochondria in Δ*taz1* yeast, similar to ATP synthase oligomer mutants, exhibit altered cristae morphology even though ATP synthase oligomer formation is unaffected. Thus, the Taz1p interactome defined here provides novel insight into the variable respiratory defects and morphological abnormalities observed in mitochondria of BTHS patients.

INTRODUCTION

The mitochondrial inner membrane (IM) forms a barrier that not only compartmentalizes numerous critical cellular activities, including iron–sulfur cluster formation and the tricarboxylic acid cycle, but additionally maintains the electrochemical gradient established by the electron transport chain and harnessed by the ATP synthase to generate ATP. The composition of the mitochondrial IM is unique, containing a distinctively high ~3–4:1 protein:phospholipid ratio. In contrast, the mitochondrial outer membrane (OM) ratio is ~1–1.6:1 (Sperka-Gottlieb *et al.*, 1988; Ardail *et al.*, 1990; Simbeni *et al.*, 1991). The IM also contains cardiolipin (CL), the signature phospholipid of mitochondria. CL is a structurally unusual phospholipid, with one negative charge associated with its two headgroups at physiological pH and four associated fatty acyl chains (Schlame *et al.*, 2000; Haines and Dencher, 2002). CL is intimately associated with all of the major players in oxidative phosphorylation, including complexes I, III, IV, and V, and the major carrier proteins for adenine nucleotides and phosphates (Schlame *et al.*, 2000). Moreover, CL is required to fully reconstitute the activity of respiratory complex IV and the ADP/ATP carrier (AAC) in vitro (Hoffmann *et al.*, 1994; Sedlak and Robinson, 1999). In organello, CL acts as a glue that stabilizes the assembly of individual respiratory complexes into so-called respiratory supercomplexes (Zhang *et al.*, 2002, 2005; Pfeiffer *et al.*, 2003) that function to increase the efficiency of oxidative phosphorylation (Boumans *et al.*, 1998; Zhang *et al.*, 2005). Which aspect of CL (e.g., its two phosphate headgroups or four associated acyl chains) is responsible for these unique functional properties of CL is at present unknown.

Cardiolipin synthase, Crd1p, synthesizes CL in the matrix-facing leaflets of the mitochondrial IM (Schlame and Haldar, 1993). Newly synthesized CL undergoes a remodeling process, the end result of which is the incorporation of more unsaturated fatty acyl chains and the establishment of a high degree of acyl chain symmetry (Schlame *et al.*, 2005). One pathway of CL remodeling is mediated by the CL transacylase, tafazzin (Taz1p; Xu *et al.*, 2006b), the mutant gene product associated with the X-linked disease Barth syndrome (BTHS). BTHS is characterized by cardiac and skeletal myopathies and cyclic neutropenia (Barth *et al.*, 1983, 1999, 2004); the disease presents in infants and if undiagnosed, is often fatal due to cardiac failure or sepsis. There are three hallmarks of the loss of Taz1p activity in the mitochondria of BTHS patients (Vreken *et al.*, 2000; Valian-

This article was published online ahead of print in *MBC in Press* (http://www.molbiolcell.org/cgi/doi/10.1091/mbc.E08–09–0896) on September 17, 2008.

Address correspondence to: Carla M. Koehler (Koehler@chem.ucla.edu).

Abbreviations used: AAC, ADP/ATP carrier; BTHS, Barth syndrome; BN-PAGE, blue native PAGE; CL, cardiolipin; CNAP, consecutive nondenaturing affinity purification; IM, inner membrane; IMS, intermembrane space; IP, immunoprecipitation; LC-MS/MS, liquid chromatography–tandem mass spectrometry; MLCL, monolysocardiolipin; OM, outer membrane; PC, phosphatidylcholine; Taz1p, tafazzin; wt, wild-type.

© 2008 by The American Society for Cell Biology

pour *et al.*, 2002, 2005; Schlame *et al.*, 2003; Schlame and Ren, 2006): 1) CL content is reduced; 2) CL contains more randomly distributed, saturated fatty acyl chains; and 3) there is an accumulation of monolysocardiolipin (MLCL). These three characteristics have been defined in the yeast *Saccharomyces cerevisiae* BTHS model (Vaz *et al.*, 2003; Gu *et al.*, 2004; Testet *et al.*, 2005; Claypool *et al.*, 2006); all but the accumulation of MLCL has been documented in the *Drosophila melanogaster* BTHS model (Xu *et al.*, 2006a), and the mitochondrial phospholipids have not been characterized in the zebrafish BTHS model (Khuchua *et al.*, 2006). Currently, it is not known whether it is the reduced steady-state abundance, the altered profile of attached fatty acyl chains, the accumulation of MLCL, a combination of all three, or some unanticipated activity of Taz1p that results in the pathologies associated with BTHS.

Early studies on BTHS patient samples revealed alterations in mitochondrial structure (Barth *et al.*, 1983) as well as variable defects in oxidative phosphorylation (Barth *et al.*, 1983, 1996; Ades *et al.*, 1993; Christodoulou *et al.*, 1994). Importantly, the multitude of available BTHS models collectively reflects these phenotypes. Given the importance of CL in the proper functioning of many of the components of the oxidative phosphorylation machinery, a reasonable hypothesis for the defects in respiration in BTHS patients, and models alike, is that reduced CL content, altered acyl chain content, and/or the increased abundance of MLCL destabilize respiratory supercomplexes resulting in reduced respiratory efficiency. Consistent with this postulate, the assembly and stability of respiratory supercomplexes is compromised in fibroblasts derived from BTHS patients (McKenzie *et al.*, 2006) and in one yeast BTHS model (Brandner *et al.*, 2005). However, we recently demonstrated in another yeast BTHS model (a different strain than used in Brandner *et al.*, 2005), that although there are moderate but significant changes in respiratory supercomplex function, there are no discernable defects in respiratory supercomplex assembly in the absence of Taz1p (Claypool *et al.*, 2008). Thus, the root cause for the assorted respiratory defects in BTHS patients remains to be determined. The potential involvement of Taz1p in establishing and/or maintaining mitochondrial organization/ultrastructure is intriguing. Phospholipases and acyltansferases that modulate the abundance of certain classes of structural phospholipids have been hypothesized to promote membrane curvature and membrane fusion events (Chernomordik *et al.*, 2006). Interestingly, Taz1p has been localized to both the mitochondrial IM and OM always facing the intermembrane space (IMS; Claypool *et al.*, 2006). Therefore, Taz1p has the functional capacity to modulate lipids in a manner that can impact their intrinsic structural properties and is localized to regions of the mitochondrion with defining morphological features including contact sites between the IM and OM as well as the cristae of the IM.

Although much progress has been made, it remains unresolved why mutations in *TAZ1* cause the numerous phenotypes of BTHS. Are they caused by changes to CL per se? Or are they the consequence of altered functioning of a protein(s) that requires the normal steady-state form of CL and/or Taz1p for activity? Our previous work demonstrated that yeast Taz1p assembles in several distinct-sized complexes (Claypool *et al.*, 2006). Proteins and/or lipids that interact with Taz1p have not been identified. In the present study, we addressed this deficiency by determining the Taz1p interactome and the importance of CL for these interactions. The Taz1p interactome defined herein identifies unexpected associations that collectively provide new insight into some of the pathologies observed in BTHS patients.

MATERIALS AND METHODS

Yeast Strains

All strains were derived from the wild-type (wt) parental *S. cerevisiae* yeast strain GA74-1A (*MAT a, his3-11,15, leu2, ura3, trp1, ade8, rho*$^+$, *mit*$^+$). The Δ*taz1* (*MAT a, leu2, ura3, trp1, ade8,* Δ*taz1::HISMX6*) and Δ*crd1* (*MAT a, his3-11,15, leu2, ura3, ade8,* Δ*crd1::TRP*) strains have been described (Claypool *et al.*, 2006, 2008; Claypool *et al.*, 2008). To generate the Δ*taz1*Δ*crd1* (*MAT a, leu2, ura3, ade8,* Δ*taz1::HISMX6,* Δ*crd1::TRP*) and Δ*atp2* (*MAT a, leu2, ura3, trp1, ade8,* Δ*atp2::HISMX6*) strains, the entire open reading frame of each gene was replaced using the PCR-mediated one-step gene replacement strategy (Wach *et al.*, 1994).

Molecular Biology

To place the CNAP tag (amino acid sequence: MEDQVDPIDGK-GGAGG-**HHHHHHHHHH**; the Protein C [PC] epitope tag is underlined, and the His_{10} tag is in bold) onto the N-terminus of Taz1p but still under control of the Taz1p promoter, overlap extension was performed (Ho *et al.*, 1989). The sequence of every construct was verified by DNA sequencing. The sequences of all primers are available upon request.

Antibodies

Most of the antibodies used in this work were generated in the Schatz lab or our lab and have been described previously. Other antibodies used were as follows: mouse anti-Sec62p (kind gift of Dr. David Meyers, University of California, Los Angeles), mouse anti-β actin (Abcam, Cambridge, MA), mouse anti-Myc tag (9E10; Evan *et al.*, 1985; obtained from the Developmental Studies Hybridoma Bank, developed under the auspices of the National Institute of Child Health and Human Development and maintained by the University of Iowa, Iowa City, IA), mouse anti-yAAC2 (clone 6H8; Panneels *et al.*, 2003), and mouse anti-PC (Roche, Indianapolis, IN) monoclonal antibodies, and horseradish peroxidase–conjugated secondary antibodies (Pierce, Rockford, IL).

Electron Microscopy

Conventional electron microscopy was performed as previously described (Rieder *et al.*, 1996). Briefly, the cells were fixed in 3% glutaraldehyde contained in 0.1 M Na cacodylate, pH 7.4, 5 mM $CaCl_2$, 5 mM $MgCl_2$, and 2.5% sucrose for 1 h at 25°C with gentle agitation; spheroplasted; embedded in 2% ultra-lo- temperature agarose (prepared in water); cooled; and subsequently cut into small pieces (~1 mm^3). The cells were then postfixed in 1% OsO_4/1% potassium ferrocyanide contained in 0.1 M cacodylate/5 mM $CaCl_2$, pH 7.4, for 30 min at room temp. The blocks were washed thoroughly four times with ddH_20, 10 min total; transferred to 1% thiocarbohydrazide at room temperature for 3 min; washed in ddH_2O (four times, 1 min each); and transferred to 1% OsO_4/1% potassium ferrocyanide in cacodylate buffer, pH 7.4, for an additional 3 min at room temperature. The cells are then washed four times with ddH_2O (15 min total); en bloc–stained in Kellenberger's uranyl acetate (UA) for 2 h to overnight; dehydrated through a graded series of ethanol; and subsequently embedded in Spurr resin. Sections were cut on a Reichert Ultracut T ultramicrotome; poststained with UA and lead citrate; and observed on a Philips TEM 420 microscope (Mahwah, NJ) at 80 kV. Images were recorded with a Soft Imaging Systems Megaview III digital camera (Olympus Soft Imaging Solutions, Lakewood, CO), and figures were assembled in Adobe Photoshop 10.0 (San Jose, CA).

Miscellaneous

Subcellular fractionation, isolation of mitochondria, alkali extraction, submitochondrial localization, and immunoblotting were as described (Claypool *et al.*, 2006); 2D Blue native/SDS-PAGE, consecutive nondenaturing affinity purification (CNAP), immunoprecipitation (IP), and liquid chromatography–tandem mass spectrometry (LC-MS/MS) were as described (Claypool *et al.*, 2008). The performed experiments used mitochondria harvested from yeast grown at 30°C to OD_{600} ~3 as follows: in Figures 1, 3A, 7D, and 8 and Supplemental Figure S1, rich lactate medium (1% yeast extract, 2% tryptone, 0.05% dextrose, and 2% lactic acid, 3.4 mM $CaCl_2{\cdot}2H_2O$, 8.5 mM NaCl, 2.95 mM $MgCl_2{\cdot}6H_2O$, 7.35 mM KH_2PO_4, and 18.7 mM NH_4Cl); in Figures 2, 3, B and C, 4, and 5, B and C, and in Supplemental Figures S2, S3, and S4, synthetic lactate −Leu (0.17% yeast nitrogen base minus amino acids and ammonium sulfate, 0.5% ammonium sulfate, 0.2% dropout mix synthetic minus Leu, 0.05% dextrose, and 2% lactic acid, 3.4 mM $CaCl_2{\cdot}2H_2O$, 8.5 mM NaCl, 2.95 mM $MgCl_2{\cdot}6H_2O$, 7.35 mM KH_2PO_4, and 18.7 mM NH_4Cl); and in Figures 5A, 6, and 7A, YP-dextrose. Protein synthesis was inhibited by the addition of 200 μg/ml cycloheximide for the final 4 h of growth before isolating mitochondria. Phospholipid labeling and extraction and data collection was as described (Claypool *et al.*, 2006) except that the extracted phospholipids were

resolved only one time on the thin-layer chromatography (TLC) plates. Statistical comparisons were performed utilizing SigmaStat 3 software (Jandel, San Rafael, CA).

Online Supplemental Material

Available online are Supplemental Figures S1–S4 presenting additional control studies of Taz1p in Δ*crd1* mitochondria, the phospholipid analyses of the MycTaz and TazHis$_8$Taz constructs, subcellular and submitochondrial localization studies of CNAPTaz, and immunoblots after CNAP, respectively, and Supplemental Table S1 that presents the LC-MS/MS data generated for Figure 4.

RESULTS

Altered Membrane Association and Complex Formation of Taz1p in the Absence of CL

CL is required for the assembly, stability, and/or function of numerous proteins and protein complexes resident to the mitochondrial IM (Schlame *et al.*, 2000). Taz1p is a phospholipid transacylase that can utilize MLCL as acyl chain acceptor (Xu *et al.*, 2006b) and localizes to both the IM and OM, always facing the IMS (Claypool *et al.*, 2006). Therefore, we wanted to determine the importance of CL on the expression, localization, membrane association, and complex assembly of Taz1p. In Δ*crd1* mitochondrial lipid extracts, CL was not detected and the precursor phospholipid in CL biosynthesis, phosphatidylglycerol (PG), amassed. In Δ*taz1* extracts, the abundance of CL decreased and MLCL, the intermediate in the CL remodeling pathway, accumulated (Figure 1A). A Taz1p immunoblot of whole cell extracts suggested that the absolute expression level of Taz1p was not affected by the presence or absence of its target phospholipid, CL (Supplemental Figure S1A). A more quantitative analysis of the mitochondrial expression of Taz1p demonstrated that Taz1p levels were statistically the same regardless of whether mitochondrial membranes contained CL (Figure 1B). Equal mitochondrial expression of Taz1p in the context of CL-containing or CL-deficient membranes implies that CL is not a determinant of proper mitochondrial targeting by Taz1p. Additionally, based on a similar proteinase K sensitivity profile as Tim54p (IM protein with large domain residing in IMS), Taz1p still associated with mitochondrial membranes that line the IMS in Δ*crd1* mitochondria (Supplemental Figure S1B).

Yeast Taz1p associates with mitochondrial membranes via an unusual membrane anchor that protrudes into, but not all the way through, the lipid bilayer (Claypool *et al.*, 2006). This type of integral interfacial membrane association is biochemically indistinguishable from classical integral membrane proteins when performing alkali extraction. Alkali extraction is used to distinguish between integral (retained in pellet) and peripheral (released into supernatant) membrane proteins. In fact, when applied over a pH range, integral membrane proteins are released into the supernatant providing a signature alkali extraction profile for each protein. Interestingly, the alkali extraction profile of Taz1p was different in Δ*crd1* than wt mitochondria (Supplemental Figure S1C). Specifically, Taz1p was significantly less extractable at pH 11.5 in the absence versus the presence of CL (Figure 1C). This was not a general feature as the extraction profile of Tim23p (four transmembrane domains) was the same in wt and Δ*crd1* mitochondria. The assembly of Taz1p into complexes was analyzed by 2D blue native/SDS-PAGE (BN/SDS-PAGE; Figure 1D). In the presence or absence of CL, the majority of Taz1p resolved at or below 67 kDa, likely reflecting a Taz1p monomer (44 kDa); however, several discrete larger complexes were readily detected. Intriguingly, a very large Taz1p-containing complex (highlighted by red arrow) was only observed in wt mitochondrial extracts and not in either Δ*crd1* or Δ*taz1* extracts. Whether the absence of this largest complex explains the distinct alkali extraction profiles of Taz1p in wt and Δ*crd1* mitochondria is unclear. Thus, in the absence of CL, the membrane association and complex assembly of Taz1p is altered.

Taz1p Does Not Form Homodimers

On the basis of migration as determined by 1D BN-PAGE, Brandner *et al.* (2005) suggested that Taz1p might assemble as a homodimer. To determine if Taz1p does in fact form homodimers, a differential epitope-tagging strategy was used. Specifically, Δ*taz1* yeast expressing either MycTaz (Myc tag on N–terminus) or TazHis$_8$Taz (His$_8$ within coding sequence just after amino acid 154) constructs alone on high-copy (↑ copy) plasmids or coexpressing MycTaz and TazHis$_8$Taz on low-copy (↓ copy) plasmids were generated. Previously, we have demonstrated that Taz1p constructs containing epitope tags on either the N-terminus or within the Taz1p-coding sequence just after aa 154 are expressed at equivalent levels and functional (Claypool *et al.*, 2006); indeed based on the lack of accumulation of MLCL, MycTaz and TazHis$_8$Taz were functional (Supplemental Figure S2). Importantly, MycTaz and TazHis$_8$Taz assembled normally when expressed alone or coexpressed (Figure 2A), indicating that the Taz1p interactome was preserved for each Taz1p variant. To determine if Taz1p does form homodimers, TazHis$_8$Taz was affinity-purified by Ni^{2+}NTA chromatography, and bound material was analyzed by immunoblot for total Taz1p or MycTaz (Figure 2B). When expressed individually, TazHis$_8$Taz but not MycTaz bound to the Ni^2 resin, as expected. When coexpressed, none of the bound Taz1p contained a Myc tag. Thus, we conclude that yeast Taz1p does not form homodimers.

To confirm this conclusion, we determined whether a previously characterized BTHS mutant tafazzin, G230R, acted in a dominant-negative manner when expressed in the context of endogenous Taz1p (Figure 2C). As BTHS is X-linked, the absence of a female carrier with disease symptoms is explained by X-chromosome inactivation. Thus, the ability of a mutant Taz1p to interfere with wt Taz1p function has not been documented. Of the four BTHS mutations that we have characterized, the G230R mutant was selected because, in contrast to the three other mutants that are mislocalized to the mitochondrial matrix, the G230R BTHS mutant is still resident to IMS-facing membranes (Claypool *et al.*, 2006). Consistent with the conclusion that Taz1p does not function as an obligate homodimer, the G230R BTHS mutant does not act in a dominant-negative manner when coexpressed with endogenous Taz1p.

Taz1p Associates with AAC2 and the ATP Synthase in Distinct Complexes

Because Taz1p assembled in several distinct complexes and the largest complex either depends on CL for its stability or represents a physical association between Taz1p and Crd1p, we defined the Taz1p interactome. A yeast strain lacking both the *TAZ1* and *CRD1* genes (Δ*taz1*Δ*crd1*) was generated. Analysis and quantitation of the mitochondrial phospholipid profile in the Δ*taz1*Δ*crd1* strain demonstrated that the Δ*taz1*Δ*crd1* strain phenocopied the Δ*crd1* strain (Figure 3A). This had been expected but never previously demonstrated and is consistent with Taz1p acting downstream of Crd1p. Second, we appended onto the N-terminus of Taz1p, but still under control of the Taz1p promoter, the recently developed consecutive nondenaturing affinity purification (CNAP; pronounced k∂ nap) tag (Claypool *et al.*, 2008). Importantly, CNAPTaz retained function (Figure 3B), cofractionated with

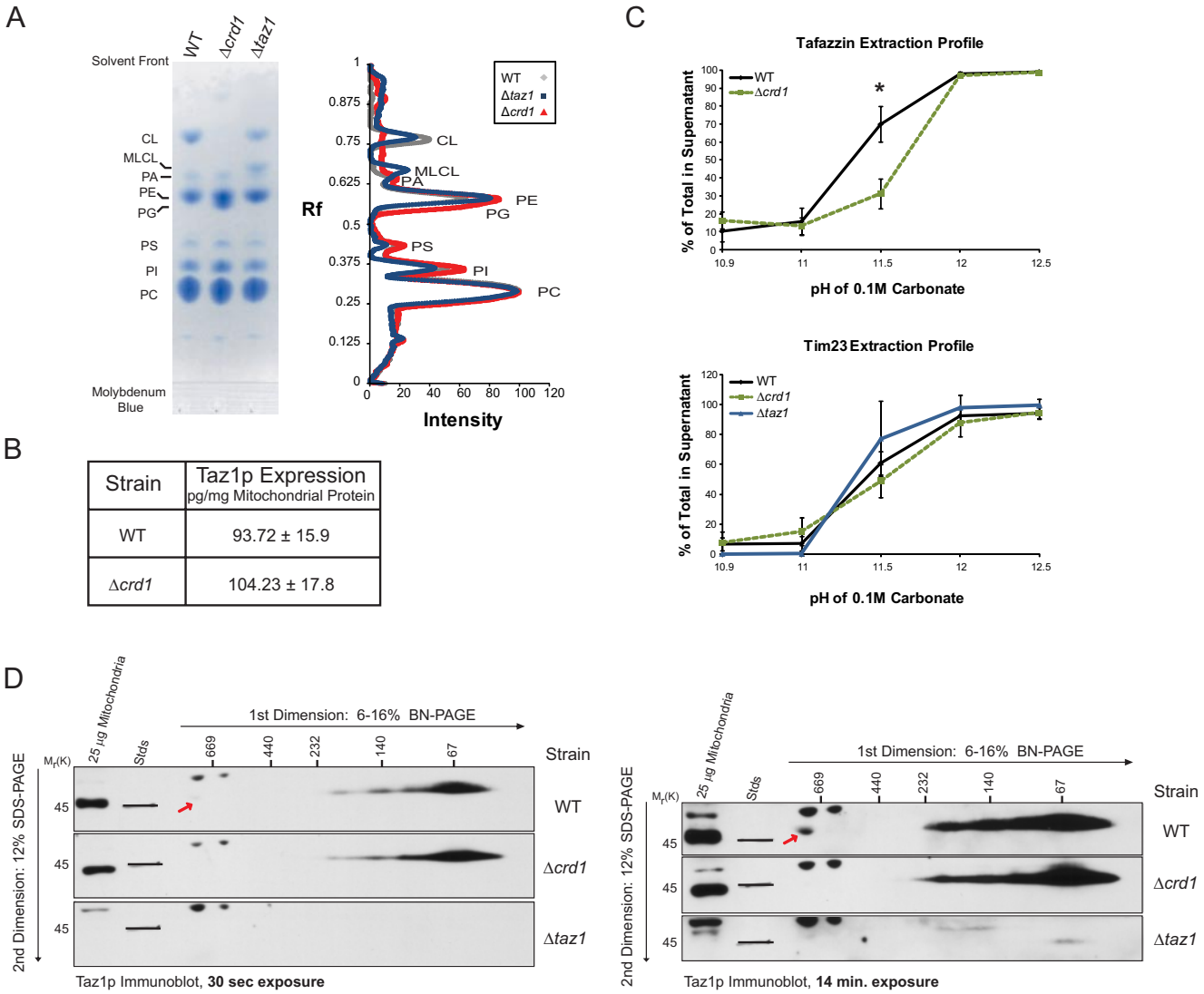

B

Strain	Taz1p Expression pg/mg Mitochondrial Protein
WT	93.72 ± 15.9
Δ*crd1*	104.23 ± 17.8

Figure 1. Altered membrane association and complex formation of Taz1p in absence of CL. (A) Phospholipids were extracted from 1 mg of mitochondria isolated from the indicated strains and separated by TLC, and phospholipids were visualized using molybdenum blue. Scanned images were analyzed using Quantity 1 software and lane analyses functions. The determined phospholipid profile for each mitochondrial sample was calculated after background correction. The migration of phospholipids is indicated; PC, phosphatidylcholine; PI, phosphatidylinositol; PS, phosphatidylserine; PE, phosphatidylethanolamine; PA, phosphatidic acid. (B) Quantification of Taz1p levels in mitochondria was determined by immunoblot using a recHis$_6$Taz standard curve (mean ± SEM, n = 4). (C) WT or Δ*crd1* mitochondria were analyzed by alkali extraction using 0.1 M carbonate at the indicated pH values. Equal volumes of the pellet (P) and TCA-precipitated supernatant (S) fractions were immunoblotted for the indicated mitochondrial markers. Bio-Rad (Richmond, CA) Versadoc-captured images were quantified using the affiliated Quantity 1 software and the percent Taz1p or Tim23p present in the derived supernatants after extraction in carbonate at each pH determined as follows: S/(S+P) × 100, where S is the volume of protein detected in the supernatant at a given pH and P is the volume associated with the pellet at the same pH. The asterisks indicates a statistically significant difference in the extractability of Taz1p from wt and Δ*crd1* mitochondria as calculated by the Student's t test, $p < 0.001$ (mean ± SD, n = 4–5). (D) 100 μg of 1.5% (wt/vol) digitonin extracts from mitochondria derived from the indicated strains were resolved by 2D BN/SDS-PAGE, and Taz1p complexes were revealed by immunoblot. The exposure of each set of immunoblots is designated at the bottom. n = 3.

mitochondria (Supplemental Figure S3A), and localized to mitochondrial membranes facing the IMS (Supplemental Figure S3B). Further, the assembly of CNAPTaz, either in the presence (Δ*taz1*) or absence (Δ*taz1*Δ*crd1*) of CL was similar to endogenous Taz1p (Figure 3C). Thus, CNAPTaz is physiologically relevant as it recapitulates all of the cell biological parameters established for endogenous Taz1p.

To identify associating proteins, we performed a preparative scale CNAP (schematized on the left in Figure 4). As a negative control, CNAP was performed on mitochondrial extracts containing untagged Taz1p (I, Δ*taz1*[Taz1p]). In comparison to this negative control, when CNAP was performed on extracts containing CNAPTaz and CL (II, Δ*taz1*[CNAPTaz]), numerous unique co-affinity–purified bands were detected upon SYPRO Ruby staining. The abundance of many of these copurified bands was decreased in CNAPed samples derived from extracts containing CNAPTaz but not CL (III, (Δ*taz1*Δ*crd1* [CNAPTaz1]). Surprisingly, the major ADP/ATP carrier, AAC2 (highlighted in orange) and five different subunits of the ATP synthase (blue) were identified by LC-MS/MS analysis of tryptic digests from the indicated bands. Additional proteins that

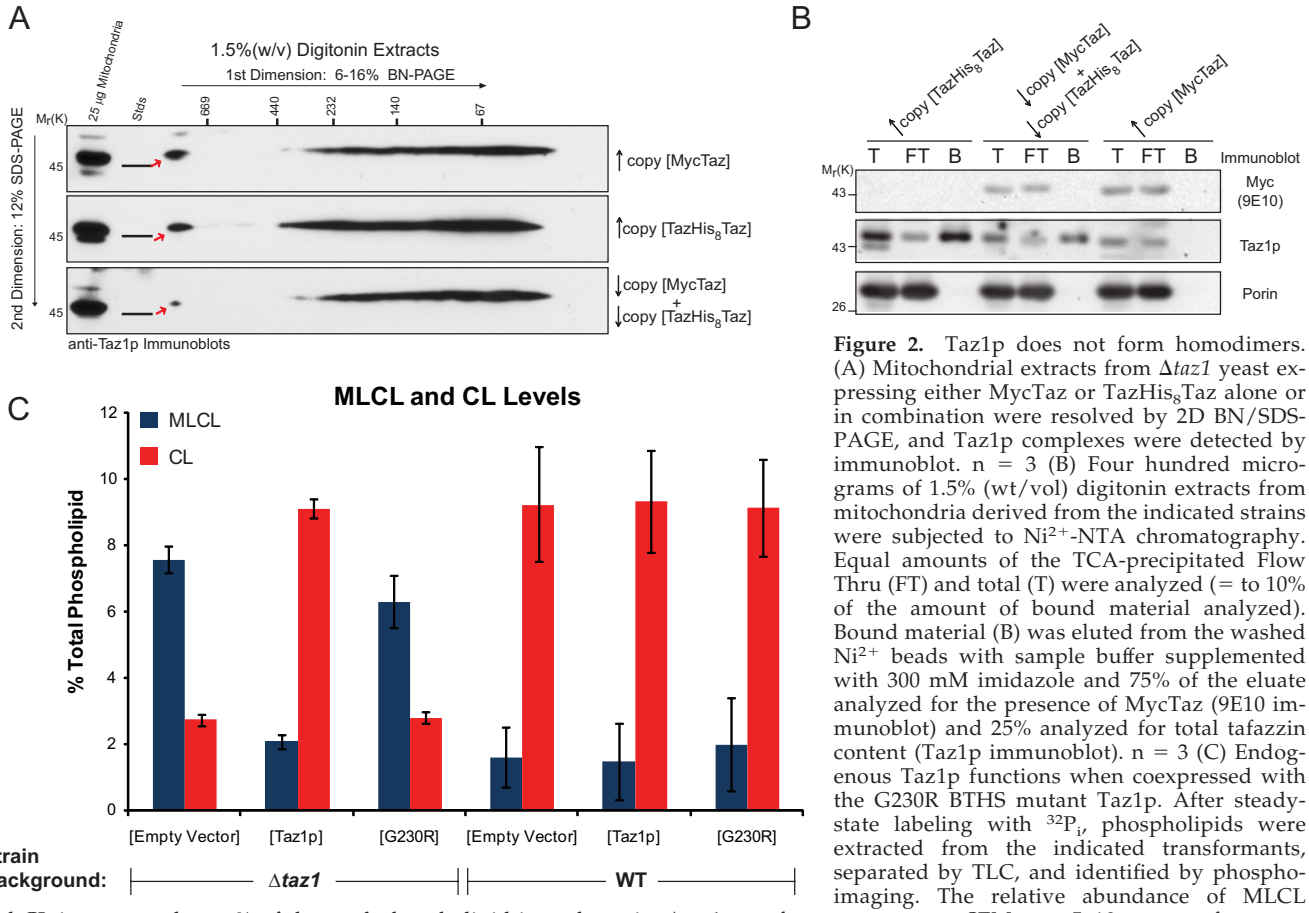

Figure 2. Taz1p does not form homodimers. (A) Mitochondrial extracts from Δ*taz1* yeast expressing either MycTaz or TazHis$_8$Taz alone or in combination were resolved by 2D BN/SDS-PAGE, and Taz1p complexes were detected by immunoblot. n = 3 (B) Four hundred micrograms of 1.5% (wt/vol) digitonin extracts from mitochondria derived from the indicated strains were subjected to Ni^{2+}-NTA chromatography. Equal amounts of the TCA-precipitated Flow Thru (FT) and total (T) were analyzed (= to 10% of the amount of bound material analyzed). Bound material (B) was eluted from the washed Ni^{2+} beads with sample buffer supplemented with 300 mM imidazole and 75% of the eluate analyzed for the presence of MycTaz (9E10 immunoblot) and 25% analyzed for total tafazzin content (Taz1p immunoblot). n = 3 (C) Endogenous Taz1p functions when coexpressed with the G230R BTHS mutant Taz1p. After steady-state labeling with $^{32}P_i$, phospholipids were extracted from the indicated transformants, separated by TLC, and identified by phosphoimaging. The relative abundance of MLCL and CL is expressed as a % of the total phospholipid in each strain. Δ*taz1* transformants, mean ± SEM, n = 5–10; wt transformants, mean ± SEM, n = 3.

copurified with CNAPTaz included three heat-shock proteins (two Hsp70 proteins, encoded by *SSC1* and *SSC3*, and Hsp60), Cor1p, and Sdh2p. These identifications were deemed likely contaminants as the proteins either reside within a different mitochondrial compartment as Taz1p (all three heat-shock proteins are resident to the matrix) or participate in multisubunit complexes and none of the other subunits of the complex were identified (Sdh2p and Cor1p are in respiratory complexes II and III, respectively).

Multiple approaches were used to independently confirm the interactions between Taz1p and AAC2 and Taz1p and the ATP synthase. First, after CNAP, the affinity-purified material was analyzed by immunoblot (Supplemental Figure S4). When membranes contained CL, CNAPTaz, but not untagged Taz1p, co-affinity–purified subunits of the ATP synthase (F1α and F1β) and a small amount of AAC, but none of the highly abundant OM protein porin. In the absence of CL, CNAPTaz still affinity-purified the ATP synthase, but AAC was no longer detected. Second, we used a mAb specific to the N-terminus of yeast AAC2 (Panneels *et al.*, 2003) to determine if endogenous Taz1p and AAC2 interact (Figure 5A). Indeed, Taz1p, but not subunits of the ATP synthase or porin, was co-immunoprecipitated (co-IP) with AAC2 from wt mitochondrial extracts. Importantly, Taz1p was not co-IPed with AAC2 in the absence of either Taz1p or AAC2 expression. Interestingly, although Taz1p was co-IPed with AAC2 from extracts lacking CL, the abundance of copurified Taz1p was reduced. The failure to co-IP the ATP synthase with AAC2 from wt mitochondrial extracts suggested that the association of Taz1p with AAC2 does not depend on, nor is it mediated through the ATP synthase. Indeed, although in reduced quantities, Taz1p was co-IPed with AAC2 from extracts lacking assembled ATP synthase (Δ*atp2*, Atp2p = F1β).

Third, the interaction of Taz1p with the ATP synthase was analyzed by co-IP immunoblot utilizing a polyclonal antiserum raised against the ATP synthase holoenzyme. Unfortunately, our Taz1p antiserum is cross-reactive to the F1α and/or F1β subunits (migrate slightly above Taz1p by SDS-PAGE) of the ATP synthase, preventing us from using this reagent to confirm this interaction with endogenous proteins. Therefore, the association of Taz1p and the ATP synthase was investigated utilizing the CNAPTaz panel. To detect the CNAPTaz constructs, an anti-PC epitope tag mAb was utilized, which as expected, failed to recognize untagged Taz1p in either the starting material or after the ATP synthase was IPed (Figure 5B). In contrast, CNAPTaz was co-IPed with the ATP synthase and the abundance of co-IPed CNAPTaz was greater when mitochondria contained CL. Critically, CNAPTaz, although readily detected, failed to be co-IPed from Δ*atp2*[CNAPTaz] extracts, demonstrating the specificity of this interaction. That AAC2 was not co-IPed with the ATP synthase from Δ*taz1*[CNAPTaz] extracts indicates that the association of Taz1p with the ATP synthase does not include AAC2.

To determine whether Taz1p associates with the ATP synthase and AAC2 in distinct complexes, the concentrated eluates after CNAP were analyzed by 2D BN/SDS-PAGE

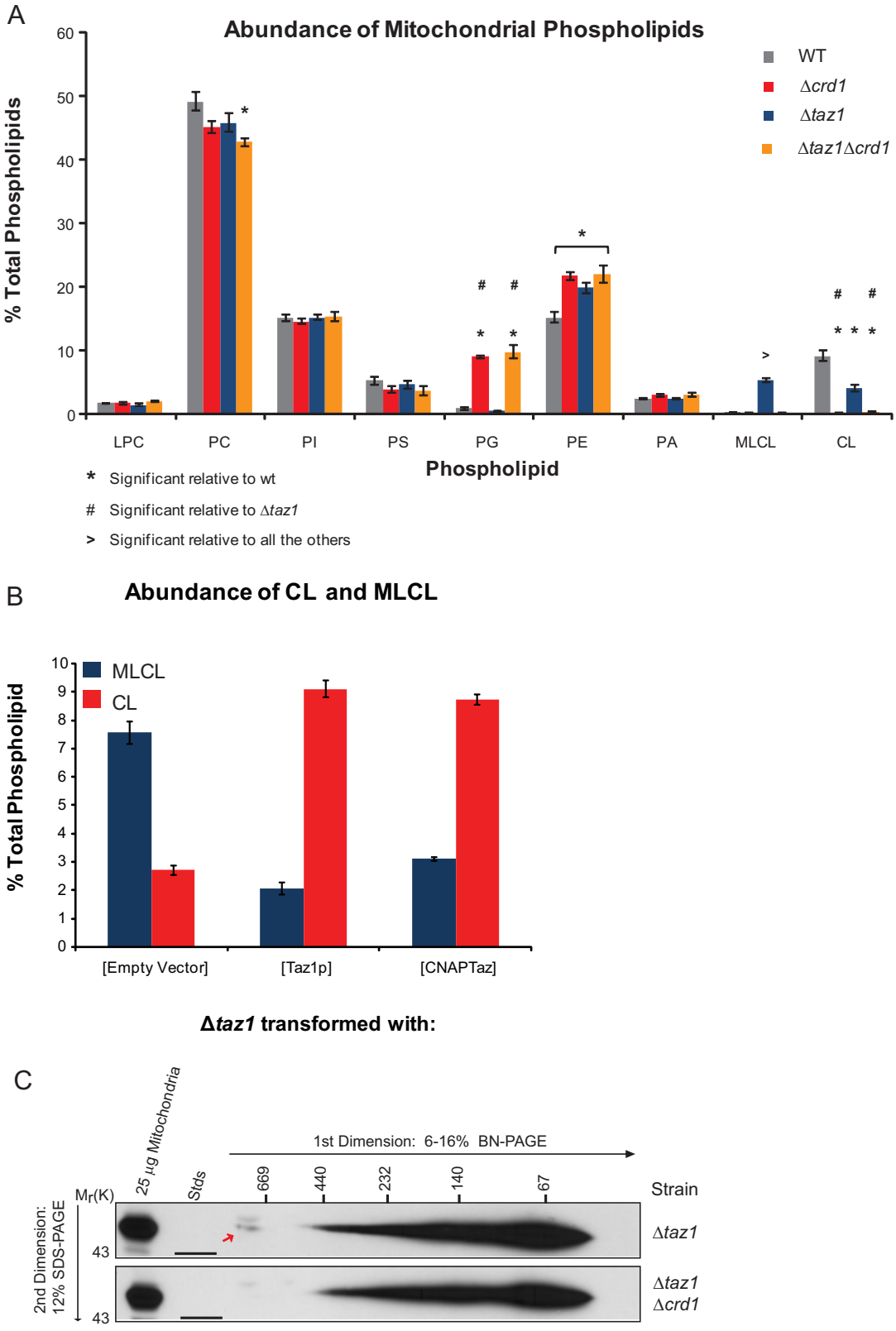

Figure 3. CNAPTaz is physiologically relevant. (A and B) Steady-state ^{32}P labeling and analyses were performed as described in Figure 2. In A, the relative abundance of each phospholipid is expressed as a % of the total phospholipid in each strain (mean ± SEM, n = 3–5). Statistical significance (p = 0.05) was determined by one-way ANOVA, with Holm-Sidak pairwise comparisons. In B, the relative abundance of MLCL and CL is expressed as a % of the total phospholipid in each strain (mean ± SEM, n = 3–10) (C) Digitonin extracts from Δ*taz1*[CNAPTaz] and Δ*taz1*Δ*crd1*[CNAPTaz] mitochondria were resolved by 2D BN/SDS-PAGE, and Taz1p complexes were detected by immunoblot. n = 3.

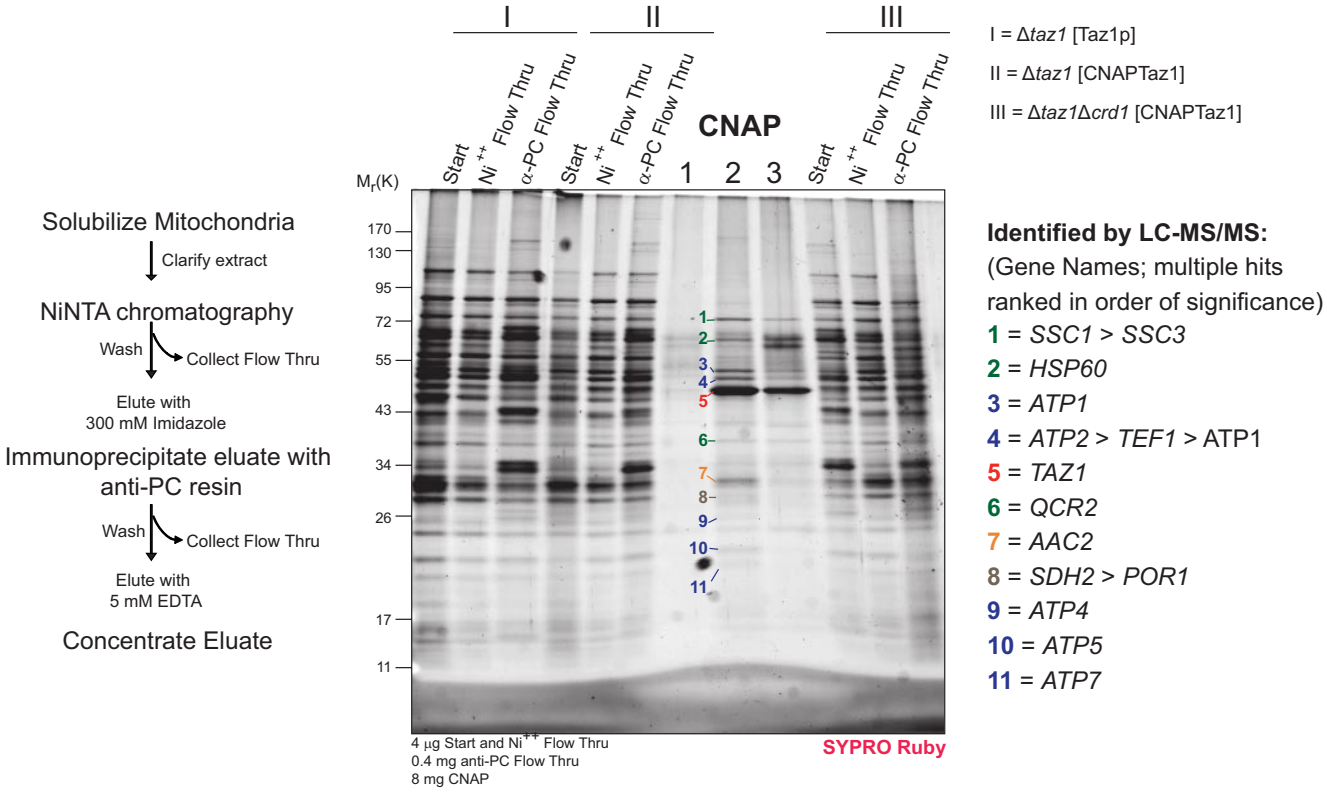

Figure 4. 1D analysis of the Taz1p interactome with and without CL. After CNAP of extracts derived from mitochondria generated from the indicated strains, the final concentrated eluates were resolved by 10–15% SDS-PAGE. SYPRO Ruby detected bands were extracted and digested with trypsin, and proteins were identified by LC-MS/MS. The *GENE* identification of the designated bands is indicated at the right.

and immunoblotting (Figure 5C). Taz1p, the ATP synthase, and AAC2 were not detected in samples derived from extracts containing untagged Taz1p and CL (top three panels), demonstrating the specificity of this approach. In marked contrast, a range of Taz1p-containing complexes were observed when extracts contained CNAPTaz and CL, including the largest Taz1p-containing complex (middle three panels). This largest Taz1p complex was not detected when CNAPTaz was affinity-purified from extracts lacking CL (bottom three panels). In addition, CNAPTaz copurified from CL-containing membranes the ATP synthase in a complex of ~600 kDa (red arrow) and AAC2 complexes that range from ~500–300 kDa (green arrows). When expressed in membranes devoid of CL, CNAPTaz still copurified a small amount of ~600-kDa ATP synthase; however, no AAC2-containing complexes were detected. The failure to detect AAC2-containing complexes in the 2D analysis was seemingly at odds with the co-IP results (Figure 5A); this most likely reflects a further destabilization of the already weakened Taz1p–AAC2 interaction during the BN-PAGE in the absence of CL. Based on the size of the ATP synthase–Taz1p complex and the fact that 5 of the 13 ATP synthase subunits were identified by LC-MS/MS, we conclude that Taz1p physically associates with the assembled ATP synthase. Thus, Taz1p participates in at least two distinct protein complexes, one consisting of assembled ATP synthase and another that includes AAC2. Further, based on the co-IP data (Figure 5, A and B), both associations are stabilized by, but do not absolutely require, CL.

Probing the Functional Relevance of the Defined Taz1p Interactome

To begin to dissect the functional significance of the established Taz1p interactome, we analyzed the expression level (Figure 6A) and assembly status (Figure 6B) of the ATP synthase and AAC2 in assorted yeast mutants. Because both AAC2 and the ATP synthase are required for growth on respiratory media, the mitochondria used in this analysis were isolated from strains grown with dextrose as the carbon source. The expression level (Figure 6A) and assembly status (Figure 6B, top panels) of the ATP synthase was not altered by the absence of Taz1p, Crd1p, or AAC2. Similarly, the expression level and complex assembly of AAC2 was not changed when mitochondria lack either Taz1p or the ATP synthase (bottom panels). As previously demonstrated, AAC2 complex formation was drastically dependent on CL and the largest AAC2 complex, representing AAC2 associated with respiratory supercomplexes, was not detected in *rho*− mitochondria (Claypool *et al.*, 2008). Thus, Taz1p is not required for the proper expression and/or assembly of the ATP synthase or the range of AAC2-containing complexes.

Taz1p expression was the same in wt mitochondria as in mitochondria lacking CL, AAC2, Atp2p (F1β), or the mitochondrial genome (*rho*−; Figure 6A). Intriguingly, in Δ*atp2* and *rho*− mitochondria, both of which fail to assemble ATP synthase dimers or monomers (Figure 6B, *top panels*), but not in Δ*aac2* mitochondria, the largest Taz1p complex was not detected (Figure 7A). Although this is consistent with the interpretation that the largest Taz1p-containing complex represents the Taz1p–ATP synthase complex, this conclusion is clouded by the observation that the largest Taz1p

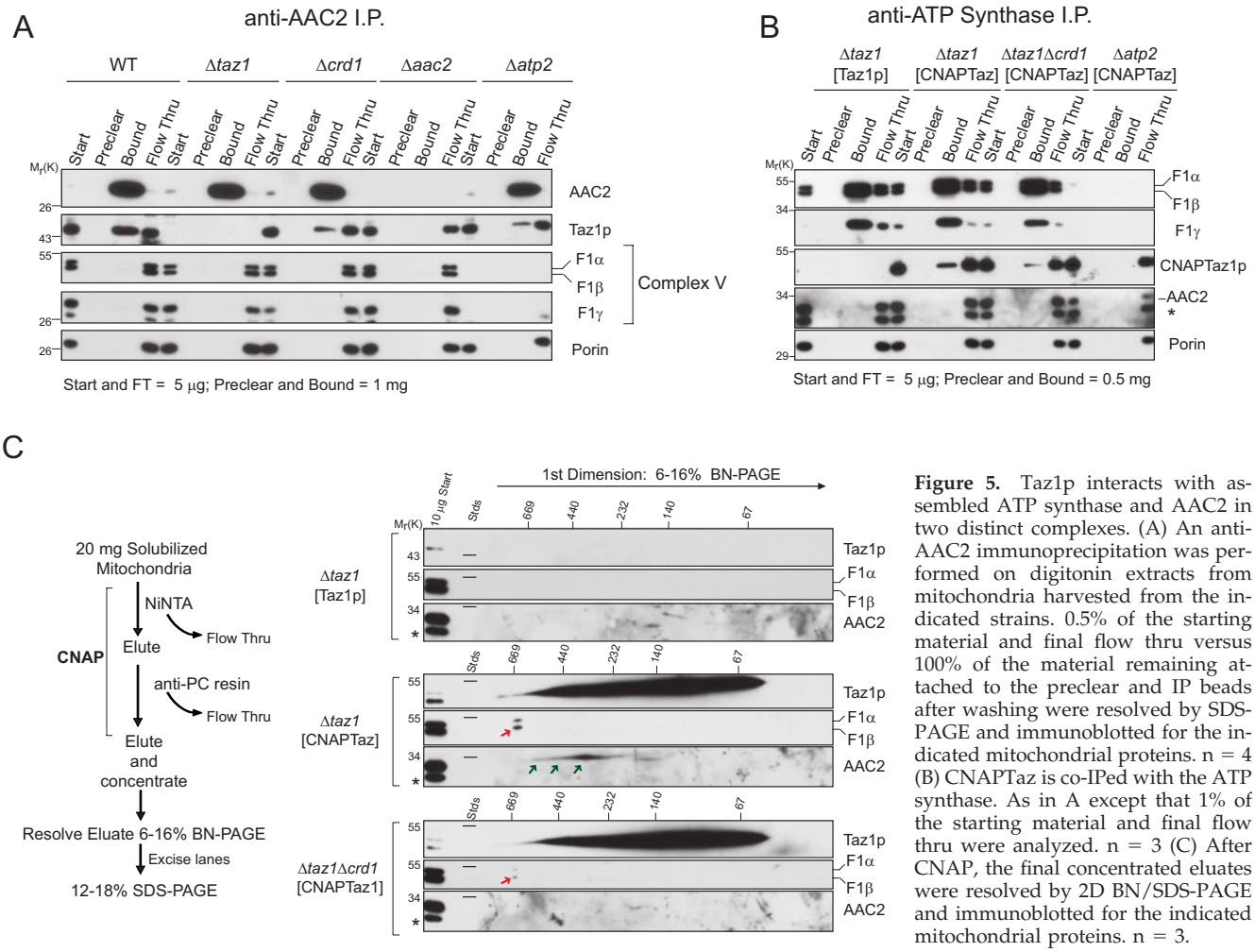

Figure 5. Taz1p interacts with assembled ATP synthase and AAC2 in two distinct complexes. (A) An anti-AAC2 immunoprecipitation was performed on digitonin extracts from mitochondria harvested from the indicated strains. 0.5% of the starting material and final flow thru versus 100% of the material remaining attached to the preclear and IP beads after washing were resolved by SDS-PAGE and immunoblotted for the indicated mitochondrial proteins. n = 4 (B) CNAPTaz is co-IPed with the ATP synthase. As in A except that 1% of the starting material and final flow thru were analyzed. n = 3 (C) After CNAP, the final concentrated eluates were resolved by 2D BN/SDS-PAGE and immunoblotted for the indicated mitochondrial proteins. n = 3.

complex was only very weakly detected in mitochondrial extracts derived from wt yeast grown in dextrose. To determine if the ability to detect the largest Taz1p complex was influenced by the carbon source used to grow the wt yeast, we directly compared Taz1p complexes in dextrose- and lactate-derived wt mitochondria (Figure 7B). Indeed, the largest Taz1p complex was readily detected in the lactate-derived wt extracts compared with the dextrose-derived wt mitochondrial extracts. Notably, mitochondria grown in dextrose versus lactate contained significantly less CL (Figure 7C), as reported previously (Gu *et al.*, 2004; Chen *et al.*, 2008). Therefore, whether the large Taz1p complex requires a certain threshold of CL for its stability or the abundance of the large Taz1p complex is below the level of detection in dextrose-derived mitochondrial extracts is unclear.

Next, we sought to determine if the observed Taz1p complexes represent stable or transient assemblies. To this end, we isolated mitochondria from wt yeast grown in lactate medium supplemented with the translation inhibitor, cycloheximide (CHX). Comparison by 2D BN/SDS-PAGE demonstrated that all of the Taz1p complexes, as well as the ATP synthase and AAC2 complexes, were still observed even if protein synthesis was blocked for 4 h (Figure 7D). This indicates that all of the detected Taz1p complexes represent final associations as opposed to intermediate steps in the ultimate assembly of a single Taz1p complex.

Oligomers of the ATP synthase have been demonstrated to be critical in establishing and maintaining normal cristae morphology (Paumard *et al.*, 2002; Goyon *et al.*, 2008; Strauss *et al.*, 2008). To gain insight into the functional relevance of the Taz1p–ATP synthase association, we analyzed wt and Δ*taz1* yeast by electron microscopy (Figure 8). Unlike the wt strain, which always had normal mitochondrial profiles with well-defined cristae (Figure 8, A and B), Δ*taz1* mitochondria often had dramatic alterations in IM structure, with profiles containing circular arrays or elongated cristae (Figure 8, C–F). The aberrant IM structures were often greater than 1 μm in length. Strikingly, the altered mitochondrial morphologies observed in the Δ*taz1* yeast were similar to those reported for ATP synthase oligomer mutants (Paumard *et al.*, 2002; Goyon *et al.*, 2008) even though ATP synthase oligomerization was normal in the absence of Taz1p (Figure 6B).

DISCUSSION

Whereas mutations in *TAZ1* result in BTHS, why either the absence of Taz1p or the expression of BTHS mutant tafazzins result in the numerous pathologies associated with BTHS remains largely a mystery. To begin to address this critical issue, we focused our efforts on defining the Taz1p interactome. The importance of CL in the defined interac-

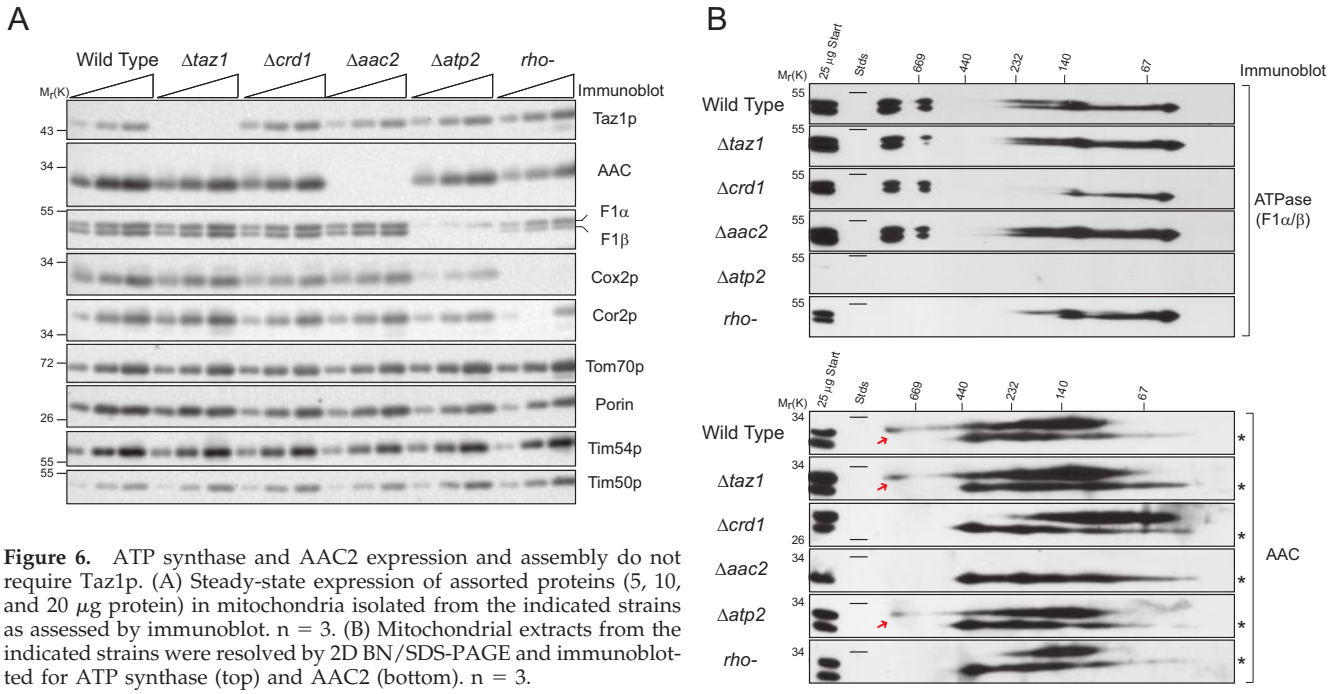

Figure 6. ATP synthase and AAC2 expression and assembly do not require Taz1p. (A) Steady-state expression of assorted proteins (5, 10, and 20 μg protein) in mitochondria isolated from the indicated strains as assessed by immunoblot. n = 3. (B) Mitochondrial extracts from the indicated strains were resolved by 2D BN/SDS-PAGE and immunoblotted for ATP synthase (top) and AAC2 (bottom). n = 3.

tome was additionally addressed because we demonstrated that in the absence of CL, the membrane association of Taz1p is subtly but significantly altered and a very large Taz1p complex is missing. A prerequisite to identifying Taz1p-interacting proteins was to address the possibility that, as suggested (Brandner *et al.*, 2005), Taz1p associates with itself. In fact, we demonstrated using two distinct strategies that yeast Taz1p does not form homodimers. Instead, Taz1p participates in at least two distinctly sized complexes of different subunit composition. Specifically, Taz1p associates with assembled ATP synthase and separately with AAC2 in complexes that range in size from ~500 to 300 kDa. The conclusion that the Taz1p–ATP synthase and Taz1p–AAC2 complexes are distinct is based on the following observations: 1) endogenous Taz1p was co-IPed with AAC2 in a strain lacking assembled ATP synthase; 2) the ATP synthase was not co-IPed with AAC2 from wt extracts; 3) AAC2 was not co-IPed with the ATP synthase even though CNAPTaz was; 4) 2D BN/SDS-PAGE analysis of CNAPed samples demonstrated that CNAPTaz copurified an ATP synthase complex of ~600 kDa, likely representing the monomeric form, and several AAC2-containing complexes that range from ~500 to 300 kDa; and 5) the largest Taz1p complex was not detected in mitochondrial extracts lacking assembled ATP synthase but was detected in the absence of AAC2. Although this last point is obscured to some degree because of the decreased ability to detect the largest Taz1p complex in mitochondria isolated from dextrose-grown wt yeast relative to lactate-grown wt yeast, the bulk of the data are consistent with the conclusion that the largest Taz1p complex corresponds to Taz1p-ATP synthase.

Worth noting, the vast majority of Taz1p was resolved by 2D BN/SDS-PAGE from ~67 to 232 kDa and thus clearly represents Taz1p not associated with either AAC2 or the ATP synthase. There are at least two possible explanations for our failure to identify the nature of these most abundant Taz1p complexes. First, the unidentified proteins that participate in these low-molecular-weight Taz1p complexes may not be detected by the used proteomic strategy (SDS-PAGE followed by LC-MS/MS). It is well documented that different proteomic strategies provide distinct information (Reinders *et al.*, 2006); thus complimentary downstream analyses after CNAP may facilitate identification of these partner proteins. Second, the low-molecular-weight Taz1p complexes may represent Taz1p in association with phospholipids and/or their derivatives. Phospholipid analyses after CNAP should provide insight into this possibility.

AAC2 and the ATP synthase are functionally interrelated. AAC2 mediates the 1:1 exchange of ADP_{in} and ATP_{out} across the mitochondrial IM. Thus, AAC2 provides the substrate, ADP that is utilized by the ATP synthase to produce ATP. Once produced, ATP is transported across the IM by AAC2 in exchange for ADP. Both AAC2 and the ATP synthase are structurally associated with CL (Beyer and Klingenberg, 1985; Eble *et al.*, 1990; Nury *et al.*, 2005) as opposed to simply embedded in membranes that happen to contain CL. Very little is known about how so-called structural phospholipids are incorporated into the final tertiary and/or quaternary structure of membrane proteins. Is this a passive process that occurs coincident with nascent protein folding/assembly or instead does it represent an active process mediated by a protein that loads phospholipids into the correct final destination? If it is the latter, then in the absence of this activity, proteins that require it for their proper folding and assembly might display altered expression and/or aberrant formation of complexes. As a phospholipid transacylase, we hypothesized that Taz1p might facilitate the proper insertion of phospholipids into the final assembled ATP synthase and assorted AAC2 complexes. As the steady-state expression and complex assembly of the ATP synthase and AAC2 did not depend on Taz1p expression, this hypothesis is likely not correct, a conclusion further supported by the stability of the Taz1p, AAC2, and ATP synthase complexes even when protein synthesis is blocked.

So what is Taz1p doing in the context of the two defined interactions? In stark contrast to the ATP synthase that seems undeterred by the absence of CL, assembly of AAC2 into normal complexes is drastically altered when mitochon-

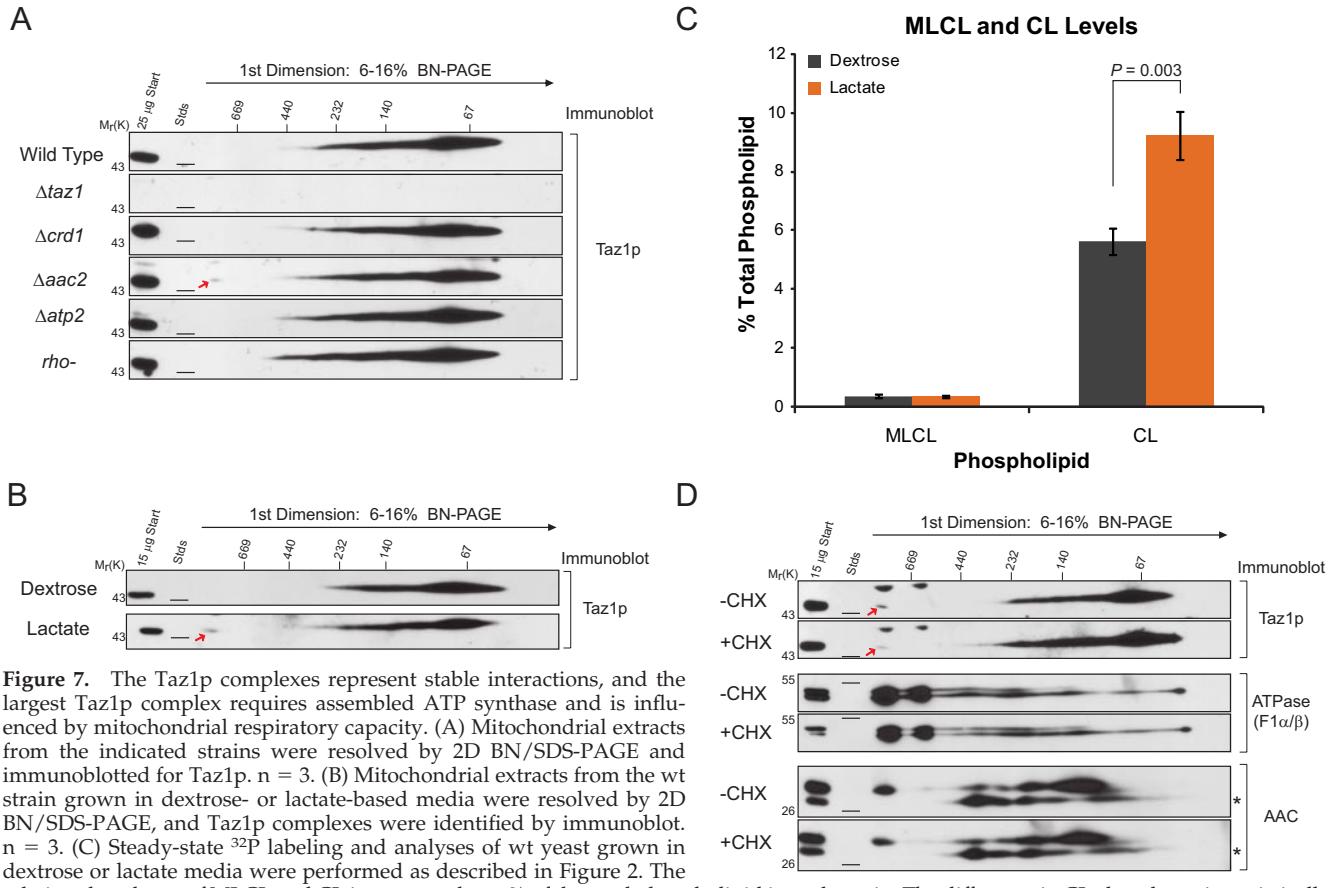

Figure 7. The Taz1p complexes represent stable interactions, and the largest Taz1p complex requires assembled ATP synthase and is influenced by mitochondrial respiratory capacity. (A) Mitochondrial extracts from the indicated strains were resolved by 2D BN/SDS-PAGE and immunoblotted for Taz1p. n = 3. (B) Mitochondrial extracts from the wt strain grown in dextrose- or lactate-based media were resolved by 2D BN/SDS-PAGE, and Taz1p complexes were identified by immunoblot. n = 3. (C) Steady-state ^{32}P labeling and analyses of wt yeast grown in dextrose or lactate media were performed as described in Figure 2. The relative abundance of MLCL and CL is expressed as a % of the total phospholipid in each strain. The difference in CL abundance is statistically significant as calculated by the Student's *t* test, p = 0.003 (mean ± SEM, n = 5–6). (D) WT yeast were grown in lactate medium and where indicated, 200 µg/ml cycloheximide (+CHX) was added for the final 4 h of growth before mitochondrial isolation. Mitochondrial extracts were resolved by 2D BN/SDS-PAGE and immunoblotted for Taz1p (top panels), ATP synthase (middle panels), and AAC2 (bottom panels). n = 3.

drial membranes lack CL (Figure 6B; Claypool *et al.*, 2008). In addition, AAC function depends on CL, both in vitro and in vivo (Hoffmann *et al.*, 1994; Jiang *et al.*, 2000; Claypool *et al.*, 2008). Moreover, CL peroxidation inactivates mammalian AAC resulting in apoptosis (Imai *et al.*, 2003). The electron transport chain is known to be the major source of reactive oxygen species, and CL, because of its high degree of unsaturation, is particularly sensitive to oxidative damage. Therefore, it is tempting to speculate that Taz1p might preserve AAC function subsequent to peroxidation of CL structurally associated with AAC. If true, deficits in AAC function could underlie the variable oxidative phosphorylation defects observed in BTHS patients. Additionally, this would indicate that Taz1p not only establishes, but also maintains, the normal fatty acyl chain profile of CL. Unfortunately, this is a difficult issue to address at present, a fact that primarily reflects the three aforementioned hallmarks of the complete loss of Taz1p function. In the absence of Taz1p, CL levels are reduced (variable 1), the remaining CL contains random more saturated fatty acyl chains (decreased sensitivity to oxidative damage, variable 2), and MLCL accumulates (variable 3). Acquisition of a temperature-sensitive Taz1p mutant would remove these variables from the equation and allow this potential function of Taz1p to be addressed.

Early studies on patient biopsies (Barth *et al.*, 1983), as well as more recent analyses using electron tomography (Acehan *et al.*, 2007), indicate that mitochondrial ultrastructure is abnormal in BTHS tissues and cells. Specifically, mitochondrial size is more variable, giant mitochondria more abundant, and, similar to our observations (Figure 8, C–F), cristae morphology is altered in the absence of Taz1p activity. CL is a so-called structural phospholipid capable of adopting lamellal or inverted hexagonal structures depending on the presence of divalent cations (Ortiz *et al.*, 1999). Taz1p, as a transacylase, can actually perform this function in either direction, i.e., it can transfer an acyl chain from PC to MLCL and from CL to lyso-PC (Xu *et al.*, 2006b). Although the PC–CL transacylase activity is the highest, Taz1p can catalyze reversible transacylations between PE and CL, PC and PE, and PC and PA (Xu *et al.*, 2006b). PE and CL are both cone-shaped phospholipids that exhibit negative spontaneous curvature; lyso-PC, an inverted cone-shaped lipid, exhibits positive spontaneous curvature (Chernomordik and Kozlov, 2005). Thus, Taz1p has the ability to modify multiple classes of phospholipid that, because of their inherent structure, have been implicated in membrane curving and fusion events (Chernomordik *et al.*, 2006). Our prior localization of Taz1p to all IMS-facing membranes is consistent with the hypothesis that Taz1p participates in enzymatic cascades that promote the establishment and maintenance of a mechanistically unexplained morphological feature of mitochondria, namely contact sites between the IM and OM.

Our identification that Taz1p interacts with assembled ATP synthase offers additional insight into how Taz1p may participate in shaping mitochondria. Work in yeast and mammalian systems has demonstrated a critical role for

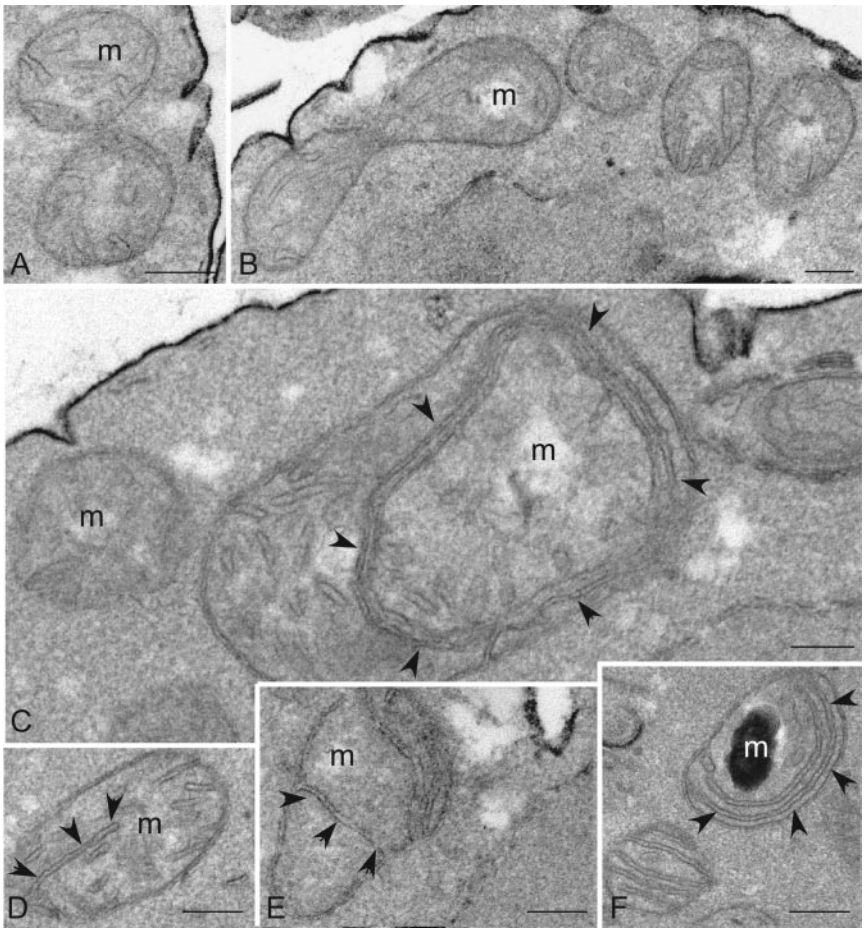

Figure 8. Morphological analysis of Δ*taz1* mitochondria by conventional TEM shows occasional swollen mitochondria and hypertrophied/aberrant cristae profiles. (A and B) WT mitochondria demonstrate a normal cristae profile. (C–F) Δ*taz1* mitochondria are occasionally swollen and have extended/hypertrophied cristae formation. m, mitochondria; arrowheads delineate hypertrophied cristae profiles in Δ*taz1*. Bars, 0.2 μm.

ATP synthase oligomers in establishing and maintaining normal cristae morphology (Paumard *et al.*, 2002; Goyon *et al.*, 2008; Strauss *et al.*, 2008). A very exciting possible function for Taz1p-ATP synthase is that Taz1p, because of its lipid modifying capabilities, is involved in the ATP synthase–dependent establishment and maintenance of normal cristae morphology, perhaps by lowering the energy barrier required to create invaginated membrane structures. Consistent with this hypothesized function, even though ATP synthase oligomerization is like wt in the absence of Taz1p activity, cristae morphology is altered. Collectively, this indicates that ATP synthase oligomerization is required but not sufficient for normal cristae morphology. Alternatively, the reduced steady-state levels of CL and/or the increased abundance of MLCL independent of the association of Taz1p with the ATP synthase may result in the altered mitochondrial morphology observed in the absence of Taz1p. However, similar to the AAC2 interaction, a concrete definition of the functional relevance of the association of Taz1p with the ATP synthase is prevented by the trifecta of alterations observed in mitochondrial membranes lacking Taz1p activity.

As CL is known to increase the efficiency of oxidative phosphorylation at least in part through its ability to promote the association of respiratory complexes into higher order supercomplexes (Boumans *et al.*, 1998; Zhang *et al.*, 2002; Pfeiffer *et al.*, 2003; Zhang *et al.*, 2005; Claypool *et al.*, 2008), the majority of studies performed to date to characterize Barth syndrome have focused on determining the importance of CL remodeling, and thus Taz1p activity, for full CL function. Our present demonstration that Taz1p physically associates with two distinct respiratory components suggests that the variable respiratory defects observed in BTHS patients may be caused by absent physical associations of Taz1p with either AAC2 and/or the ATP synthase and not secondary to alterations in the CL profile in BTHS patient mitochondria. As such, unexpected insight into many of the observed abnormalities associated with BTHS mitochondria, including variable defects in oxidative phosphorylation and altered mitochondrial ultrastucture, was provided by the presently defined yeast Taz1p interactome.

ACKNOWLEDGMENTS

We thank Dr. Jeff Schatz (University of Basel, Basel, Switzerland) for antibodies and Dr. Irmgard Sinning (University of Heidelberg, Heidelberg, Germany) for the anti-AAC2 monoclonal antibodies. This work was supported by the American Heart Association Grant 0640076N, Muscular Dystrophy Association (4033), and National Institutes of Health Grants 1R01GM61721 (C.M.K.), R01RR20004 (J.A.L.), and K99HL089185–01 (S.M.C.). The UCLA Mass Spectrometry and Proteomics Technology Center was established with a grant from the W. M. Keck Foundation. C.M.K. is an Established Investigator of the American Heart Association.

REFERENCES

Acehan, D., Xu, Y., Stokes, D. L., and Schlame, M. (2007). Comparison of lymphoblast mitochondria from normal subjects and patients with Barth syndrome using electron microscopic tomography. Lab. Invest. *87*, 40–48.

Ades, L. C., Gedeon, A. K., Wilson, M. J., Latham, M., Partington, M. W., Mulley, J. C., Nelson, J., Lui, K., and Sillence, D. O. (1993). Barth syndrome: clinical features and confirmation of gene localisation to distal Xq28. Am. J. Med. Genet. *45*, 327–334.

Ardail, D., Privat, J. P., Egret-Charlier, M., Levrat, C., Lerme, F., and Louisot, P. (1990). Mitochondrial contact sites. Lipid composition and dynamics. J. Biol. Chem. *265*, 18797–18802.

Barth, P. G., Scholte, H. R., Berden, J. A., Van der Klei-Van Moorsel, J. M., Luyt-Houwen, I. E., Van 't Veer-Korthof, E. T., Van der Harten, J. J., and Sobotka-Plojhar, M. A. (1983). An X-linked mitochondrial disease affecting cardiac muscle, skeletal muscle and neutrophil leucocytes. J. Neurol. Sci. *62*, 327–355.

Barth, P. G., Valianpour, F., Bowen, V. M., Lam, J., Duran, M., Vaz, F. M., and Wanders, R. J. (2004). X-linked cardioskeletal myopathy and neutropenia (Barth syndrome): an update. Am. J. Med. Genet. A *126*, 349–354.

Barth, P. G., Van den Bogert, C., Bolhuis, P. A., Scholte, H. R., van Gennip, A. H., Schutgens, R. B., and Ketel, A. G. (1996). X-linked cardioskeletal myopathy and neutropenia (Barth syndrome): respiratory-chain abnormalities in cultured fibroblasts. J. Inherit. Metab. Dis. *19*, 157–160.

Barth, P. G., Wanders, R. J., Vreken, P., Janssen, E. A., Lam, J., and Baas, F. (1999). X-linked cardioskeletal myopathy and neutropenia (Barth syndrome) (MIM 302060). J. Inherit. Metab. Dis. *22*, 555–567.

Beyer, K., and Klingenberg, M. (1985). ADP/ATP carrier protein from beef heart mitochondria has high amounts of tightly bound cardiolipin, as revealed by 31P nuclear magnetic resonance. Biochemistry *24*, 3821–3826.

Boumans, H., Grivell, L. A., and Berden, J. A. (1998). The respiratory chain in yeast behaves as a single functional unit. J. Biol. Chem. *273*, 4872–4877.

Brandner, K., Mick, D. U., Frazier, A. E., Taylor, R. D., Meisinger, C., and Rehling, P. (2005). Taz1, an outer mitochondrial membrane protein, affects stability and assembly of inner membrane protein complexes: implications for Barth Syndrome. Mol. Biol. Cell *16*, 5202–5214.

Chen, S., He, Q., and Greenberg, M. L. (2008). Loss of tafazzin in yeast leads to increased oxidative stress during respiratory growth. Mol. Microbiol. *68*, 1061–1072.

Chernomordik, L. V., and Kozlov, M. M. (2005). Membrane hemifusion: crossing a chasm in two leaps. Cell *123*, 375–382.

Chernomordik, L. V., Zimmerberg, J., and Kozlov, M. M. (2006). Membranes of the world unite! J. Cell Biol. *175*, 201–207.

Christodoulou, J., McInnes, R. R., Jay, V., Wilson, G., Becker, L. E., Lehotay, D. C., Platt, B. A., Bridge, P. J., Robinson, B. H., and Clarke, J. T. (1994). Barth syndrome: clinical observations and genetic linkage studies. Am. J. Med. Genet. *50*, 255–264.

Claypool, S. M., McCaffery, J. M., and Koehler, C. M. (2006). Mitochondrial mislocalization and altered assembly of a cluster of Barth syndrome mutant tafazzins. J. Cell Biol. *174*, 379–390.

Claypool, S. M., Oktay, Y., Boontheung, P., Loo, J. A., and Koehler, C. M. (2008). Cardiolipin defines the interactome of the major ADP/ATP carrier protein of the mitochondrial inner membrane. J. Cell Biol. *182*, 937–950.

Eble, K. S., Coleman, W. B., Hantgan, R. R., and Cunningham, C. C. (1990). Tightly associated cardiolipin in the bovine heart mitochondrial ATP synthase as analyzed by 31P nuclear magnetic resonance spectroscopy. J. Biol. Chem. *265*, 19434–19440.

Evan, G. I., Lewis, G. K., Ramsay, G., and Bishop, J. M. (1985). Isolation of monoclonal antibodies specific for human c-myc proto-oncogene product. Mol. Cell Biol. *5*, 3610–3616.

Goyon, V., Fronzes, R., Salin, B., di-Rago, J.-P., Velours, J., and Brethes, D. (2008). Yeast cells depleted in Atp14p Fail to assemble Atp6p within the ATP synthase and exhibit altered mitochondrial cristae morphology. J. Biol. Chem. *283*, 9749–9758.

Gu, Z., Valianpour, F., Chen, S., Vaz, F. M., Hakkaart, G. A., Wanders, R. J., and Greenberg, M. L. (2004). Aberrant cardiolipin metabolism in the yeast taz1 mutant: a model for Barth syndrome. Mol. Microbiol. *51*, 149–158.

Haines, T. H., and Dencher, N. A. (2002). Cardiolipin: a proton trap for oxidative phosphorylation. FEBS Lett. *528*, 35–39.

Ho, S. N., Hunt, H. D., Horton, R. M., Pullen, J. K., and Pease, L. R. (1989). Site-directed mutagenesis by overlap extension using the polymerase chain reaction. Gene *77*, 51–59.

Hoffmann, B., Stockl, A., Schlame, M., Beyer, K., and Klingenberg, M. (1994). The reconstituted ADP/ATP carrier activity has an absolute requirement for cardiolipin as shown in cysteine mutants. J. Biol. Chem. *269*, 1940–1944.

Imai, H., Koumura, T., Nakajima, R., Nomura, K., and Nakagawa, Y. (2003). Protection from inactivation of the adenine nucleotide translocator during hypoglycaemia-induced apoptosis by mitochondrial phospholipid hydroperoxide glutathione peroxidase. Biochem. J. *371*, 799–809.

Jiang, F., Ryan, M. T., Schlame, M., Zhao, M., Gu, Z., Klingenberg, M., Pfanner, N., and Greenberg, M. L. (2000). Absence of cardiolipin in the crd1 null mutant results in decreased mitochondrial membrane potential and reduced mitochondrial function. J. Biol. Chem. *275*, 22387–22394.

Khuchua, Z., Yue, Z., Batts, L., and Strauss, A. W. (2006). A zebrafish model of human Barth syndrome reveals the essential role of tafazzin in cardiac development and function. Circ. Res. *99*, 201–208.

McKenzie, M., Lazarou, M., Thorburn, D. R., and Ryan, M. T. (2006). Mitochondrial respiratory chain supercomplexes are destabilized in Barth Syndrome patients. J. Mol. Biol. *361*, 462–469.

Nury, H., Dahout-Gonzalez, C., Trezeguet, V., Lauquin, G., Brandolin, G., and Pebay-Peyroula, E. (2005). Structural basis for lipid-mediated interactions between mitochondrial ADP/ATP carrier monomers. FEBS Lett. *579*, 6031–6036.

Ortiz, A., Killian, J. A., Verkleij, A. J., and Wilschut, J. (1999). Membrane fusion and the lamellar-to-inverted-hexagonal phase transition in cardiolipin vesicle systems induced by divalent cations. Biophys. J. *77*, 2003–2014.

Panneels, V., Schussler, U., Costagliola, S., and Sinning, I. (2003). Choline head groups stabilize the matrix loop regions of the ATP/ADP carrier ScAAC2. Biochem. Biophys. Res. Commun. *300*, 65–74.

Paumard, P., Vaillier, J., Coulary, B., Schaeffer, J., Soubannier, V., Mueller, D. M., Brethes, D., di Rago, J. P., and Velours, J. (2002). The ATP synthase is involved in generating mitochondrial cristae morphology. EMBO J. *21*, 221–230.

Pfeiffer, K., Gohil, V., Stuart, R. A., Hunte, C., Brandt, U., Greenberg, M. L., and Schagger, H. (2003). Cardiolipin stabilizes respiratory chain supercomplexes. J. Biol. Chem. *278*, 52873–52880.

Reinders, J., Zahedi, R. P., Pfanner, N., Meisinger, C., and Sickmann, A. (2006). Toward the complete yeast mitochondrial proteome: multidimensional separation techniques for mitochondrial proteomics. J. Proteome Res. *5*, 1543–1554.

Rieder, S. E., Banta, L. M., Kohrer, K., McCaffery, J. M., and Emr, S. D. (1996). Multilamellar endosome-like compartment accumulates in the yeast vps28 vacuolar protein sorting mutant. Mol. Biol. Cell *7*, 985–999.

Schlame, M., and Haldar, D. (1993). Cardiolipin is synthesized on the matrix side of the inner membrane in rat liver mitochondria. J. Biol. Chem. *268*, 74–79.

Schlame, M., Kelley, R. I., Feigenbaum, A., Towbin, J. A., Heerdt, P. M., Schieble, T., Wanders, R. J., DiMauro, S., and Blanck, T. J. (2003). Phospholipid abnormalities in children with Barth syndrome. J. Am. Coll. Cardiol. *42*, 1994–1999.

Schlame, M., and Ren, M. (2006). Barth syndrome, a human disorder of cardiolipin metabolism. FEBS Lett. *580*, 5450–5455.

Schlame, M., Ren, M., Xu, Y., Greenberg, M. L., and Haller, I. (2005). Molecular symmetry in mitochondrial cardiolipins. Chem. Phys. Lipids *138*, 38–49.

Schlame, M., Rua, D., and Greenberg, M. L. (2000). The biosynthesis and functional role of cardiolipin. Prog. Lipid Res. *39*, 257–288.

Sedlak, E., and Robinson, N. C. (1999). Phospholipase A(2) digestion of cardiolipin bound to bovine cytochrome c oxidase alters both activity and quaternary structure. Biochemistry *38*, 14966–14972.

Simbeni, R., Pon, L., Zinser, E., Paltauf, F., and Daum, G. (1991). Mitochondrial membrane contact sites of yeast. Characterization of lipid components and possible involvement in intramitochondrial translocation of phospholipids. J. Biol. Chem. *266*, 10047–10049.

Sperka-Gottlieb, C. D., Hermetter, A., Paltauf, F., and Daum, G. (1988). Lipid topology and physical properties of the outer mitochondrial membrane of the yeast, *Saccharomyces cerevisiae*. Biochim. Biophys. Acta *946*, 227–234.

Strauss, M., Hofhaus, G., Schroder, R. R., and Kuhlbrandt, W. (2008). Dimer ribbons of ATP synthase shape the inner mitochondrial membrane. EMBO J. *27*, 1154–1160.

Testet, E., Laroche-Traineau, J., Noubhani, A., Coulon, D., Bunoust, O., Camougrand, N., Manon, S., Lessire, R., and Bessoule, J. J. (2005). Ypr140wp, 'the yeast tafazzin', displays a mitochondrial lysophosphatidylcholine (lyso-PC) acyltransferase activity related to triacylglycerol and mitochondrial lipid synthesis. Biochem. J. *387*, 617–626.

Valianpour, F. *et al.* (2005). Monolysocardiolipins accumulate in Barth syndrome but do not lead to enhanced apoptosis. J. Lipid Res. *46*, 1182–1195.

Valianpour, F., Wanders, R. J., Barth, P. G., Overmars, H., and van Gennip, A. H. (2002). Quantitative and compositional study of cardiolipin in platelets by electrospray ionization mass spectrometry: application for the identification of Barth syndrome patients. Clin. Chem. *48*, 1390–1397.

Vaz, F. M., Houtkooper, R. H., Valianpour, F., Barth, P. G., and Wanders, R. J. (2003). Only one splice variant of the human TAZ gene encodes a functional protein with a role in cardiolipin metabolism. J. Biol. Chem. *278*, 43089–43094.

Vreken, P., Valianpour, F., Nijtmans, L. G., Grivell, L. A., Plecko, B., Wanders, R. J., and Barth, P. G. (2000). Defective remodeling of cardiolipin

and phosphatidylglycerol in Barth syndrome. Biochem. Biophys. Res. Commun. *279*, 378–382.

Wach, A., Brachat, A., Pohlmann, R., and Philippsen, P. (1994). New heterologous modules for classical or PCR-based gene disruptions in *Saccharomyces cerevisiae*. Yeast *10*, 1793–1808.

Xu, Y., Condell, M., Plesken, H., Edelman-Novemsky, I., Ma, J., Ren, M., and Schlame, M. (2006a). A *Drosophila* model of Barth syndrome. Proc. Natl. Acad. Sci. USA *103*, 11584–11588.

Xu, Y., Malhotra, A., Ren, M., and Schlame, M. (2006b). The enzymatic function of tafazzin. J. Biol. Chem. *281*, 39217–39224.

Zhang, M., Mileykovskaya, E., and Dowhan, W. (2002). Gluing the respiratory chain together. Cardiolipin is required for supercomplex formation in the inner mitochondrial membrane. J. Biol. Chem. *277*, 43553–43556.

Zhang, M., Mileykovskaya, E., and Dowhan, W. (2005). Cardiolipin is essential for organization of complexes III and IV into a supercomplex in intact yeast mitochondria. J. Biol. Chem. *280*, 29403–29408.